Magnetic Resonance Imaging 59 (2019) 31–38

Contents lists available at ScienceDirect

Magnetic Resonance Imaging

journal homepage: www.elsevier.com/locate/mri

Original contribution

Feasibility of quantitative MR-perfusion imaging to monitor treatment response after uterine artery embolization (UAE) in symptomatic uterus fibroids☆

Maliha Sadick[a], Jakob Richers[a], Benjamin Tuschy[b], Lothar R. Schad[c], Stefan O. Schoenberg[a], Frank G. Zöllner[c,*]

[a] Institute of Clinical Radiology and Nuclear Medicine, University Medical Center Mannheim, Medical Faculty Mannheim, Heidelberg University, Theodor-Kutzer Ufer 1-3, 68167 Mannheim, Germany
[b] Department of Gynaecology and Obstetrics, University Medical Center Mannheim, Medical Faculty Mannheim, Heidelberg University, Theodor-Kutzer Ufer 1-3, 68167 Mannheim, Germany
[c] Computer Assisted Clinical Medicine, Medical Faculty Mannheim, Heidelberg University, Theodor-Kutzer Ufer 1-3, 68167 Mannheim, Germany

ARTICLE INFO

Keywords:
Perfusion imaging
Magnetic resonance imaging
Uterine artery embolization
Quantitative
Treatment outcome
Minimal invasive

ABSTRACT

Introduction: In 25% of women, symptomatic uterus myomas are diagnosed with clinical and functional impairment ranging from abdominal and pelvic pain to dys- and hypermenorrhea, dyspareunia, pollakiuria and infertility. Women undergoing a treatment increasingly prefer nowadays minimal invasive, uterus preserving therapies like uterine artery embolization (UAE) over surgical hysterectomy, nowadays. To emphasize the efficacy of UAE as a uterus preserving treatment with targeted therapy of myomas only, analysis of tissue perfusion pre and post embolization is required. The purpose of this study was to assess treatment response in UAE in females with symptomatic uterus myomas by quantitative magnetic resonance perfusion imaging.

Methods: Seven females scheduled for uterus myoma embolization underwent three MRI examinations (pre, post, follow-up) including morphological and dynamic contrast enhanced perfusion imaging at 3 T. To measure tumor volume, regions-of-interest covering the tumor and the uterus were drawn by two readers in consensus. Blood flow, blood volume, and mean transit time were calculated by a pixel-by-pixel deconvolution approach. Kruskal-Wallis/Friedman test was employed to test whether the group medians differ significantly with correction for multiple comparisons using Bonferroni method.

Results: Change of volume could be observed in all patients after embolization but was significantly different only between pre/post and follow-up time point. Measured differences in all perfusion parameters were significant between pre-intervention and post-intervention/follow-up in the myomas, no significant differences could be detected for the uterus tissue.

Conclusions: Our results demonstrate devascularization of symptomatic myomas which correlates with cessation of hypermenorrhea in all treated patients without affecting healthy uterus tissue. Supplementing UAE with perfusion imaging to monitor early treatment response is feasible and might provide valuable information for the follow-up of patients and contribute to providing confidence for the patients in treatment success.

1. Introduction

Uterine fibroids, also known as uterus myomas, represent the most common benign tumor of the female reproductive system and affect almost 5 to 70% of women between 30 and 50 years of age [1,2]. In most of the women, uterine fibroids do not cause any symptoms and are usually detected in routine ultrasound. In 25% of women, symptomatic uterus myomas are diagnosed with clinical und functional impairment ranging from abdominal and pelvic pain, to dys- and hypermenorrhea, dyspareunia, pollakiuria and infertility [3,4].

Abbreviations: UAE, uterine artery embolization; MRI, magnetic resonance imaging; DCE, dynamic contrast enhanced; BF, blood flow; BV, blood volume; MTT, mean transit time; ROI, region of interest

☆ Key message: Supplementing UAE with quantitative perfusion imaging to monitor treatment response is feasible and might provide valuable information for the follow-up of patients and contribute to providing confidence for the patients in treatment success.

* Corresponding author.
E-mail address: frank.zoellner@medma.uni-heidelberg.de (F.G. Zöllner).

https://doi.org/10.1016/j.mri.2019.02.008
Received 7 September 2018; Received in revised form 14 February 2019; Accepted 15 February 2019

Treatment decision has to be based on several aspects that influence therapy planning, like patients' clinical requirements, physiological condition of the affected patient, patients' age and clinical experience of the treating physician [5]. Transvaginal radiofrequency ablation of myomas has been recently described [6]. Therapy effect is dependent on size, location and number of myomas and does not represent a treatment option for women with usually large symptomatic myomas. In MR-guided High-Intensity Focused Ultrasound size and number of myomas have to be considered and previous laparotomy prior has to be excluded because of potential risk of intraprocedural complications due to heating and necrosis [7,8]. Both methods should be initially considered in young patients, as there is no radiation exposure involved. Unfortunately, in the clinical work-flow, women present with multiple large myomas. In these cases uterine artery embolization can achieve good treatment outcome.

Uterine artery embolization (UAE), first published by Ravina et al. in 1995 even currently represents an effective minimal invasive therapeutic approach for the management of symptomatic uterus fibroids [9]. With the recent ongoing discussion on liver failure in women under treatment with ulipristal acetate for symptomatic uterine fibroids even more attention should be directed towards established minimal invasive treatment options which represent a sure alternative to surgery [10,11]. Also, women undergoing a treatment increasingly prefer nowadays minimal invasive, uterus preserving therapies like UAE over surgical hysterectomy nowadays.

In initial clinical assessment and identification of myomas, ultrasound is considered a standard approach, as it is frequently available and cost effective for baseline evaluation. Diagnostic information may be limited in obese patients and large uterine fibroids [12]. The most precise imaging modality for evaluation of size, number, extension and characteristics of uterine fibroids with regard to vascularization and necrosis, remains contrast enhanced (CE) magnetic resonance imaging (MRI) [13–17]. It also enables differentiation between fibroids and potential malignant tumors and is an objective tool for characterization of volume reduction and alteration of perfusion dynamics not only in malignant, but also benign tumors, independent of size, location and vascularization of the lesions [16,18,19]. Furthermore, in pre-interventional imaging, MRI is of great benefit for analysis of arterial supply to the myomas, for assessment of individual anatomy of the uterine artery branches and to rule out variants of arterial supply which might make UAE difficult or impossible [20,21]. However, in the assessment of treatment response, the value of tumor volume estimation by CE-MRI is unclear [18].

To emphasize the efficacy of UAE as a uterus perfusion preserving treatment with targeted therapy of myomas only, quantitative perfusion parameter analysis pre and post embolization are required. So far, dynamic contrast enhanced (DCE) MRI was proposed and signal enhancement patterns were semi-quantitatively described [22].

The purpose of this study was to show the feasibility of quantitative MR perfusion imaging for the assessment of treatment response in uterine artery embolization (UAE).

2. Materials and methods

2.1. Patients

Females with symptomatic uterine fibroids consulting our Interventional Radiology outpatient clinic, mainly by self-referral and occasionally by gynaecological referral, were enrolled in our study. Patients' clinical history displayed sonographic features of enlarged myomas causing hypermenorrhagia with iron deficiency anemia due to prolonged monthly menstrual bleeding, pollakiuria and abdominal discomfort. Symptoms were assessed and documented in patients' consent sheet for UAE during outpatient consultation. Laboratory findings and evidence of iron deficiency anemia were recorded prior to UAE. Patients who had previously undergone surgery for uterine fibroids were excluded from the study. Further exclusion criteria were a potential malignant uterine finding and postmenopausal status with bleeding episodes, suspicious of a potentially underlying malignant gynaecological tumor with further investigation required. In patients with the intention to get pregnant, the ethics committee and the gynaecological board decision voted for hormonal therapy or surgical myomectomy. Women under current hormonal replacement therapy were excluded because of potential bias on treatment outcome after UAE. Given the above enrollment criteria, in 2017 seven female patients (age 46 ± 3 years) scheduled for radiological minimal invasive treatment were included in this prospective study to present a technically standardized MRI examination protocol and to show the feasibility of quantitative perfusion parameters for the assessment of treatment response in UAE.

2.2. Uterine artery embolization

Uterine artery embolization was performed after oral pain medication in each patient without necessity of peridural or general anaesthesia. In local anaesthesia a 5 French introducer sheath (Terumo Interventional Systems, Somerset, NJ) was inserted in the right common femoral artery. A diagnostic angiography of the common and internal iliac arteries was performed with a 4 French Pigtail catheter (Cordis, USA) followed by a catheterization of the uterine artery with a 4 French Optitorque catheter (Terumo Interventional Systems, Somerset, NJ). At this position superselective approach to each uterine artery was achieved with the Embocath plus microcatheter 0.028″ inner diameter (Merit Medical, Merit Medical Europe, Netherlands). Embolization was performed with 700–900-μm Embospheres (Merit Medical, Merit Medical Europe, Netherlands). UAE was ceased as soon as stasis occurred in the super selectively targeted region of embolization and an angiographic verification the patency of the main stem of the uterine artery had been performed.

2.3. MR imaging

Each patient underwent three MRI examinations including morphological imaging and dynamic contrast enhanced (DCE) perfusion imaging. Baseline MRI was performed one to four weeks prior to embolization. The first follow-up MRI (second imaging) was done 4 days after embolization followed by a routine outpatient MRI control scan after approximately 174 ± 69 days (third imaging). For each MR examinations the same standard MRI protocol was applied.

All imaging was performed on a 3 T system (Magnetom Skyra, Siemens Healthineers, Erlangen, Germany) using an 18 channel body and 32 channel spine array for signal reception. T1 with and without gadolinium contrast enhancement as well as T2-weighted MR images were performed for delineation of uterus and myomas. DCE-MRI was performed for perfusion analysis.

To measure tumor volume, a 2D T1-weighted Turbo Spin Echo sequence with parameters repetition time (TR)/echo time (TE)/flip angle (FA) = 605 ms/12 ms/150°, matrix = 320 × 218 and two averages, resulting in an in plane resolution of 0.8 × 0.8 mm^2, was performed. A 2D T2-weighted Turbo Spin Echo sequence was performed with parameters TR/TE/FA = 4200 ms/108 ms/160°, matrix = 384 × 296 and two averages, resulting in an in plane resolution of 0.7 × 0.7 mm^2. In total, in both acquisitions, 29 slices with slice thickness of 4 mm and a gap between slices of 4.6 mm were acquired in axial slice orientation.

DCE-MRI was performed using a 3D T1-weighted time-resolved angiography with stochastic trajectories sequence with parameters TR/TE/FA = 2.7 ms/0.98 ms/21° and matrix = 256 × 256 and 104 slices resulting in an isotropic voxel resolution of 1.6 mm^3 [23]. TWIST view sharing was set to outer/inner sampling density of 15%/20%. Using parallel imaging (GRAPPA, PAT 3), a nominal temporal resolution of 1.5 s was achieved. A solution consisting of 0.1 mmol/kg body weight contrast agent (Dotarem, Guerbet, France) was administered after the

Fig. 1. Morphological images of one patient at pre, post-intervention and follow-up. Illustration of signal formation in myomas in T2-weighted (A–C) and T1-weighted post contrast images (D–F). Slices are recorded in coronal direction.

acquisition of five baseline images, followed by a saline flush of 10 ml. In total 88 volumes were recorded during 2 min and 12 s. Slices were acquired in coronal direction covering the female pelvis.

2.4. Tumor volume estimation

Regions-of-interest (ROI) covering the tumor and the uterus were drawn by two experienced readers, the interventional radiologist and one cross-sectional imaging specialist, in consensus in each of the morphological images at each time point using OsiriX Dicom Workstation (Pixmeo SARL, Bernex, Switzerland). Myoma selection criteria included size in descending order, clear delineation from surrounding uterine tissue and therefore optimal size and volumetric assessment. Image interpretation was performed by an interventional radiologist with > 10 years of experience in IR and an advanced diagnostic radiologist. The performing IR physician read the MRI for dedicated procedure planning prior to embolization.

For each patient up to three myomas were depicted for volumetric and perfusion assessment, using T1- and T2-weighted coronal images (see Fig. 1). T2-weighted images were valuable for delineation of perfused versus non or less enhancing degenerated myomas. According to the study by Deipolyi et al., we included enhancing and non-enhancing myomas in the volume assessment as all uterine fibroids were targeted during embolization with the intention to reduce volume in each fibroid [19]. Myomas were classified according to their intramural, submucosal or subserosal position.

2.5. Perfusion data analysis

Qualitative change in myoma and healthy tissue perfusion was assessed by visual inspection of the signal intensity curves averaged over all voxel within the tissue and myoma ROIs.

For quantitative analysis, briefly, maps of blood flow (BF), blood volume (BV) and mean transit time (MTT) were calculated by a pixel-by-pixel deconvolution approach using an in house certified OsiriX plugin (UMMPerfusion 1.5.3) [24,25]. For estimating the arterial input function, a ROI was placed in the iliac artery proximal to the branches of smaller vessels feeding the uterus and tumor with blood. All data were normalized by subtracting the mean intensity of 5 baseline volumes and a linear relationship between contrast agent concentration and signal intensities was assumed due to the low dose of the injected contrast agent.

Despite diagnosis of several myomas in the uterine tissue, for a standardized analysis purpose, in each patient data analysis was limited to three myomas that were depicted and ROIs were drawn by two readers in consensus. For reference purposes, one ROI was placed in the healthy uterus tissue and copied to each of the calculated parametric maps to extract quantitative perfusion values. This procedure was repeated for each time point.

2.6. Statistical analyses

In order to assess possible significant differences in the obtained results, the Kruskal-Wallis test was employed to evaluate whether the group medians (pre-, post-intervention and follow-up) differ [26]. Due to high variabilities in the ROI volumes at baseline, for comparing the change in volume over time, the Friedman test was employed [27]. Based on this, a post-hoc test for pairwise comparison of the group means was performed using the Bonferroni method to correct for multiple comparisons [28]. A p-value of < 0.05 was considered as significant. Statistical analysis was done using Matlab 2016a (The Mathworks, Natick, USA). Post-hoc power analysis for the given number of included patients was performed using G*Power 3.7.1 [29].

Table 1
Patient characteristics of clinical symptoms and laboratory values at baseline and after UAE. In two patients, ferritin levels were not accessed (na).

Patient	Age	Pre-intervention					Post-intervention/follow-up	
		Quick level (%)	Hemoglobine (g/dl)	Ferritin level (μg/l)	Menstruation related pain (NRS, 0–10)	Menorrhagia	Menstruation related pain (NRS, 0–10)	Menorrhagia
1	44	100	13.1	4	9.5	Yes	9,5	Yes
2	42	105	11.1	9	4	Yes	1	No
3	47	87	12.7	10	4	Yes	1	No
4	42	98	12.8	na	6	Yes	7	No
5	51	96	14.0	na	0	No	0	No
6	50	114	14.4	15	7	No	7	No
7	45	101	12.5	7	8	Yes	0	No

2.7. Ethical approval

This study was approved by our local institutional review board and written consent was obtained from all patients.

3. Results

In total 21 myomas (3 per patient, seven patients) and seven ROIs of healthy uterus tissue were analyzed.

All statistical tests had a power of at least 0.955. This implies a sufficient number of samples for this study.

3.1. Patients

Clinical symptoms assessed pre and post UAE are depicted in Table 1. Improvement of menstruation related pain was reported in three out of seven patients. Menorrhagia was reported by five patients prior to UAE while after UAE only one patient reported menorrhagia. Table 1 also reports laboratory values which were available prior to UAE.

3.2. Tumor volume

Change of volume could be observed in all patients after embolization. In healthy uterine tissue, the mean volume was 619 ± 286 ml before treatment, 548 ± 279 ml after treatment and 369 ± 221 ml at follow-up. Change in volume was significant ($p = 0.0021$). The volume of the selected three myomas varied between each other prior to the intervention but in all three cases a reduction in volume over time was observed (see Table 2). Myoma volume averaged over all three groups was 104 ± 127 ml before treatment, 99 ± 123 ml after treatment and 46 ± 60 ml at follow-up. Changes in volume were significantly different (M1: $p = 0.0021$, M2: $p = 0.0052$, M3: $p = 0.0244$). However, inspecting the differences pairwise, for all tissues only a significant difference could be observed between pre- or post-intervention and follow-up (see Table 3).

Table 3
p-Values of multiple pairwise comparisons of perfusion parameters for the three time points. $p_{pre/post}$: pre- to post-intervention, $p_{pre/follow\text{-}up}$: pre-intervention to follow-up, and $p_{post/follow\text{-}up}$: post-intervention to follow-up). U: uterus tissue, M1–M3: myoma tissue. Bonferroni-corrected for multiple comparison. A p-value < 0.05 was considered significant.

Parameter	Tissue	$p_{pre/post}$	$p_{pre/follow\text{-}up}$	$p_{post/follow\text{-}up}$
Volume	U	0.5443	0.0015	0.0975
	M1	0.5443	0.0015	0.0975
	M2	1	0.0099	0.0226
	M3	1	0.0342	0.0806
BF	U	1	1	1
	M1	0.0011	0.0040	1
	M2	0.0004	0.0049	1
	M3	0.0005	0.052	0.6645
BV	U	0.2244	1	0.74
	M1	0.0023	0.0003	1
	M2	< 0.00001	0.0172	0.2710
	M3	0.0047	0.0071	1
MTT	U	1	1	0.62
	M1	0.0103	0.0001	0.7043
	M2	0.0001	0.0067	0.9380
	M3	0.0565	0.0013	0.6244

3.3. Perfusion imaging

The effect of the embolization could also be observed visually by inspecting signal intensity time curves as well as the signal intensity of

Table 2
Measured volume and perfusion parameters given as mean and standard deviation of all patients for representative ROIs of healthy uterus (U) and myoma tissue (M1–M3). A p-value < 0.05 denotes whether the differences between all three group medians were significantly different.

Tissue	Parameters	Pre intervention	Post intervention	Follow up	p
U	Volume (ml)	618.8 ± 286	548.1 ± 279	368.9 ± 221	0.0021
	BF (ml/min/100 ml)	45.1 ± 19	32.0 ± 12	52.9 ± 31	0.18
	BV (ml/100 ml)	34.5 ± 17	24.2 ± 10	32.3 ± 22	0.195
	MTT (s)	45.4 ± 9	49.0 ± 14	39.0 ± 11	0.417
M1	Volume (ml)	166.1 ± 156	148.0 ± 159	69.2 ± 72	0.0021
	BF (ml/min/100 ml)	62.8 ± 35	12.7 ± 7	15.7 ± 8	0.0005
	BV (ml/100 ml)	41.4 ± 19	1.1 ± 1	0.9 ± 0	0.0001
	MTT (s)	47.7 ± 9	5.5 ± 4	3.0 ± 1	0.0001
M2	Volume (ml)	41.1 ± 38	50.4 ± 43	22.6 ± 36	0.0052
	BF (ml/100 ml/min)	60.9 ± 31	16.1 ± 8	20.8 ± 8	0.0003
	BV (ml/100 ml)	35.2 ± 15	0.9 ± 1	2.2 ± 2	< 0.0001
	MTT (s)	38.5 ± 11	3.7 ± 3	5.9 ± 6	0.0001
M3	Volume (ml)	24.4 ± 25	26.0 ± 27	11.7 ± 14	0.0224
	BF (ml/100 ml/min)	68.6 ± 41	10.9 ± 5	21.7 ± 8	0.0007
	BV (ml/100 ml)	37.7 ± 18	1.6 ± 2	1.3 ± 1	0.0015
	MTT (s)	44.0 ± 7	6.4 ± 5	3.3 ± 3	0.0016

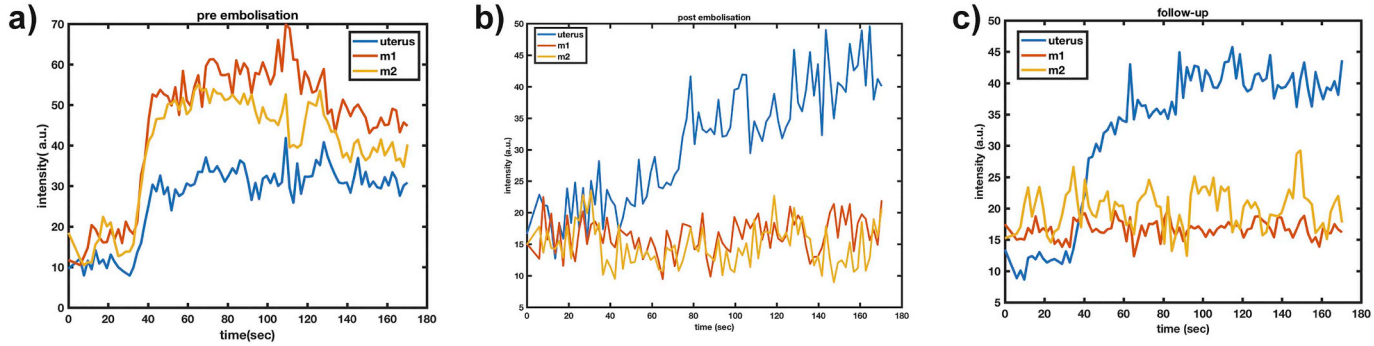

Fig. 2. Example of signal intensity time curves for healthy uterus tissue (blue) and two regions-of-interest (ROIs) of the myoma (yellow, orange) at time points: pre (a), post intervention (b), and follow up (c). Signal intensity time curves were extracted and averaged over all voxels from the same ROIs used for quantitative analysis. (For interpretation of the references to color in this figure legend, the reader is referred to the web version of this article.)

lesions in pre and post contrast morphological images. Perfusion analysis demonstrated the embolization effect on all myomas, regardless of their intramural, submucosal or subserosal location, which underlines the overall effect of UAE on all uterine fibroids, regardless of size and location, compared to other minimal invasive therapies.

Signal alteration in the morphological scans was observed, turning from initially hyperintense to hypointense lesions in the T1-weighted TSE images, appearing like “empty shells”. This supports shrinking of the lesions (see Fig. 1).

Analyzing the signal intensity time courses, for illustration purposes, Fig. 2 depicts signal intensity time curve of a healthy tissue and two lesions of one patient. Before embolization (Fig. 2a)), all three curves showed a typical perfusion pattern: flat profile before contrast agent injection, fast uptake post injection and a washout of the contrast agent thereafter. The myoma-to-treat (M1, M2) showed an even higher and faster uptake of contrast agent (steeper slope of the curves). After embolization (Fig. 2b)) and also at follow-up (Fig. 2c)) no contrast agent uptake could be detected in the myomas anymore. In contrast to the uptake patterns of myomas, in the uterus tissue a restoration of the initial perfusion pattern of the signal intensity curve could be observed. While BF and BV are limited after the intervention (slow slope of the signal intensity curve) at follow-up both parameters are restored (see Fig. 2c)).

Besides changes in volume over time, also changes in BF, BV and MTT, measured by DCE-MRI, could be detected. Fig. 3 shows the respective parametric maps for the three time points in one patient as an example. It also shows T1-weighted and T2-wheighted morphological images from matching slices depicting the ROI capturing the lesion M2. Fig. 4 depicts a boxplot of BF, BV and MTT grouped by the time point (color coded) for the ROI analysis of the myoma (M1–M3) and healthy uterus tissue (U) for all seven datasets. Except for the healthy tissue, comparing the perfusion parameters of pre-intervention to post and follow-up, the perfusion parameters are strongly reduced and the boxplots show only slight overlap at the whiskers, indicating significant differences.

In the healthy uterus tissue, the BF was on average 45.0 ± 19 ml/100 ml/min prior to the intervention, 32.0 ± 12 ml/100 ml/min after the intervention, and 52.9 ± 31 ml/100 ml/min at follow-up while for the three myomas the BF was 64.1 ± 30 ml/100 ml/min, 13.2 ± 7 ml/100 ml/min, and 19.4 ± 8 ml/100 ml/min at pre-, post-intervention and follow-up, respectively.

A similar behavior of the parameters BV and MTT could be observed. While BF and BV measured in the myomas are significantly decreased also at follow-up (all $p < 0.05$), a restoration of BF and BV is measured for the healthy uterus tissue (no significant differences of change in BF and BV between all three time points, all $p > 0.05$). The respective numbers of each patient are summarized in Table 2.

Statistical analysis revealed that no significant differences in perfusion parameters could be detected in the uterus tissue ROI (U) between pre-intervention and post-intervention/follow-up. Perfusion parameters measured in the lesions (M1–M3) differ significantly between pre-intervention and post-intervention. No significant differences in perfusion of the lesions could be observed between the post intervention and the follow-up exam (see Table 3).

4. Discussion

Magnetic resonance imaging including dynamic contrast enhanced techniques is emerging as a tool for predicting treatment response [30–33]. Contrast enhanced MRI plays an important role in the pre-interventional work-up of uterine fibroids, not only for information on size, location and extension of disease but also for procedure planning in transcatheter embolization of symptomatic myomas [34–36]. MRI is also a valuable tool for short- and long-term follow-up after UAE [20].

We are very frequently confronted with the fact, that women, who decide to go for gynaecological control ultrasound 6 to 12 months after UAE, unfortunately do not get appropriate information on the post-procedural status of myoma and uterus perfusion and decrease of size in symptomatic myomas. Especially in large fibroids exceeding 6 to 7 cm in size, ultrasound may be able to depict potentially embolized myoma shells but fails to assess vascularity of fibroids and uterus. This can have a psychological impact on the patient after UAE. Therefore, dedicated MRI imaging protocols should be applied for precise postprocedural follow-up, as they can provide objective information on myoma perfusion, devascularization and size reduction.

In this feasibility study, we showed that quantitative perfusion imaging could be used for monitoring treatment response in minimal invasive myoma embolization.

As control, we analyzed healthy uterus tissue in all patients. Although healthy uterus tissue was not targeted by the embolization particles, the perfusion immediately after the intervention and at follow-up was slightly decreased compared to the pre-intervention status, however, these changes were not significant. Perfusion values in lesions are decreased after embolization compared to those measured in pre-intervention MRI exams. At follow-up, a stronger BF is observed while MTT and BV further decrease. However, this possible reperfusion of tissue never exceeds the initial value measured prior to intervention. All measured perfusion parameters showed significant changes in the post and follow-up exam compared to the pre interventional MRI. Changes in perfusion values of post and follow-up MRI were not significant (cf. Table 3).

This can also be observed when inspecting signal intensity time curves (cf. Fig. 2). While at time point pre-intervention, all tissues showed a typical in and out flow of the contrast agent, after embolization only the healthy uterus tissue showed a contrast agent uptake. This suggests that small segmental and subsegmental arterial branches supplying the myoma were devascularized by the embolization particles and therefore no longer had any perfusion left.

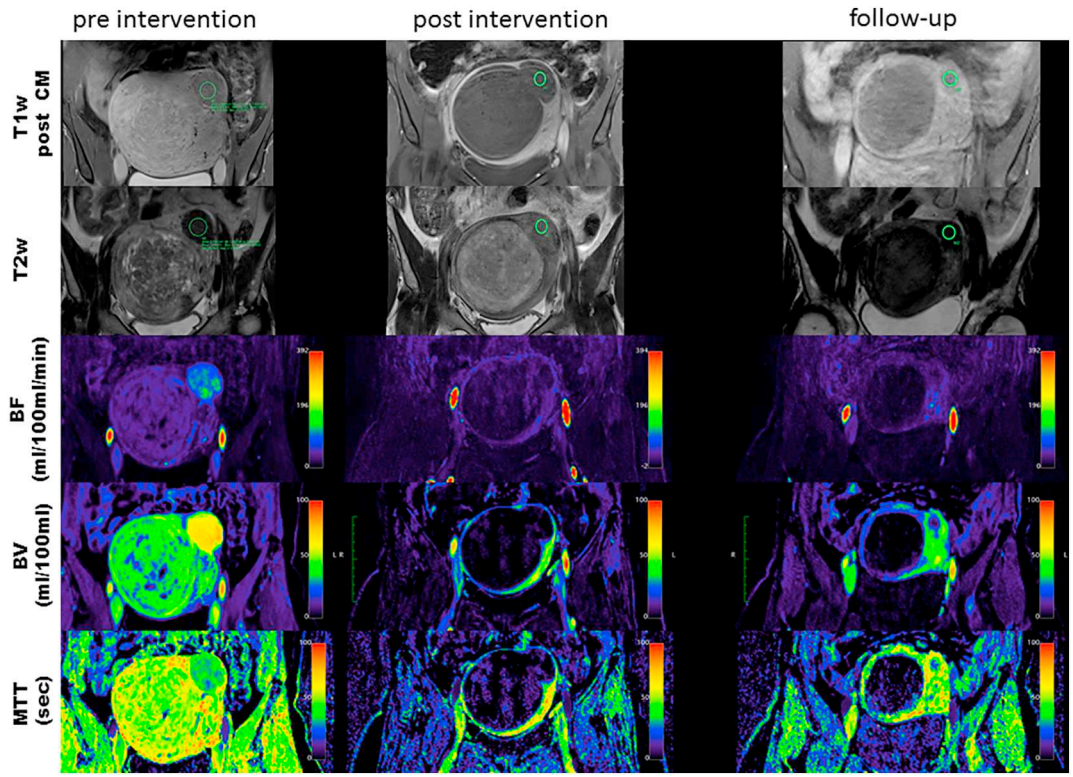

Fig. 3. Example of recorded morphological images and parametric maps calculated from the DCE-MRI exams of one patient at pre, post intervention and at follow-up. The first two rows represent a T1-weighted (T1w) and a T2-weighted (T2w) of a slice matching those of the parametric maps. At each time point, the ROI capturing the lesion M2 of this patient is depicted. The three lower rows represent one perfusion parameter each estimated using the UMMPerfusion software. Visually, in each of the three parametric maps, changes over time could be detected.

This suggests that a) the embolization was successful in all seven patients and in all targeted myomas, b) that due to the induced ischemia, the perfusion altered differently between targeted tumors and healthy (spared) tissue and c) that quantitative perfusion MRI could be well used to monitor the treatment response. The results emphasize the safety of this minimal invasive treatment technique in symptomatic uterine fibroids.

Comparing changes in tumor volume and perfusion parameters, we observed that there were significant differences immediately after embolization as far as the perfusion parameters were concerned whereas tumor volumes demonstrated no significant change in size. Further decrease in tumor volume is observed at follow-up, i.e. approximately six months after the UAE while tumor perfusion remains reduced. This might demonstrate the benefit of quantitative MR perfusion imaging for assessment of early treatment response compared to volume after UAE.

Perfusion imaging in UAE has been evaluated before, however, in these studies either a post contrast morphological image was used to assess tumor volume [20] or semi-quantitative parameters like mean peak enhancement, relative peak enhancement (to pre-interventional scan), time to peak, wash-in rate, and washout rate of the fibroids were used [37]. Li et al. described similar first pass perfusion patterns in their study as observed in our data (see Fig. 2) which supports our findings [22]. Pelage et al. also investigated long term outcome of UAE (three years after intervention) however also here no quantitative perfusion analysis was employed [17]. In contrast to these studies, to the best of our knowledge, we showed for the first time that quantitative perfusion parameters could demonstrate devascularization of symptomatic myomas depicted by a significant reduced perfusion, i.e. reduced BF, BV, and MTT. This effect is observed not only after embolization but also at follow-up while change in volume at all time points is not significant.

Comparing our results to previous studies analyzing tumor volume, we could also reproduce reduction in tumor volume [17,20]. However, significant reduction in tumor volume is only observable in the follow-up exam. This agrees with a recent study that shows limitations in the value of MRI based tumor volume estimation in treatment monitoring [18].

This study was designed as a feasibility study to evaluate if quantitative MR perfusion imaging could be used to access treatment response in minimal invasive myoma embolization. Our statistical analysis already showed strong and significant changes in the perfusion parameters that match our initial expectation on the behavior of perfusion in tissue after embolization.

A limitation was that not all lesions were analyzed but up to three myomas were selected exemplarily in each patient. Again, since this was a feasibility study, we focused on not more than three representative myomas to proof our hypothesis. An extension to analyze all detectable lesions can be performed easily since the workflow is now already established.

Furthermore, only seven patients were included. This might explain non-significant results in change of tumor volume as the standard deviation of this parameter between patients was high. Others showed significant changes in volume but had also larger cohorts [17,20,22]. However, our post hoc power analysis showed that the small number of patients was sufficient to reach enough power for our statistical tests. Also, in this study the slice thickness was rather high which could also contribute to partial volume effects and hence a larger variance in volume estimates. In future research we will optimize the morphological part and investigate whether this improve volumetry.

A correlation analysis of clinical symptoms recorded via a questionnaire and perfusion parameters was not performed due to the low number of patients. However, most patients reported a reduction of menorrhagia and some improvement in menstruation related pain while in all cases a reduction in perfusion in the myomas was observed. This gives rise to the opinion that a correlation might exists, however, a proof remains future work.

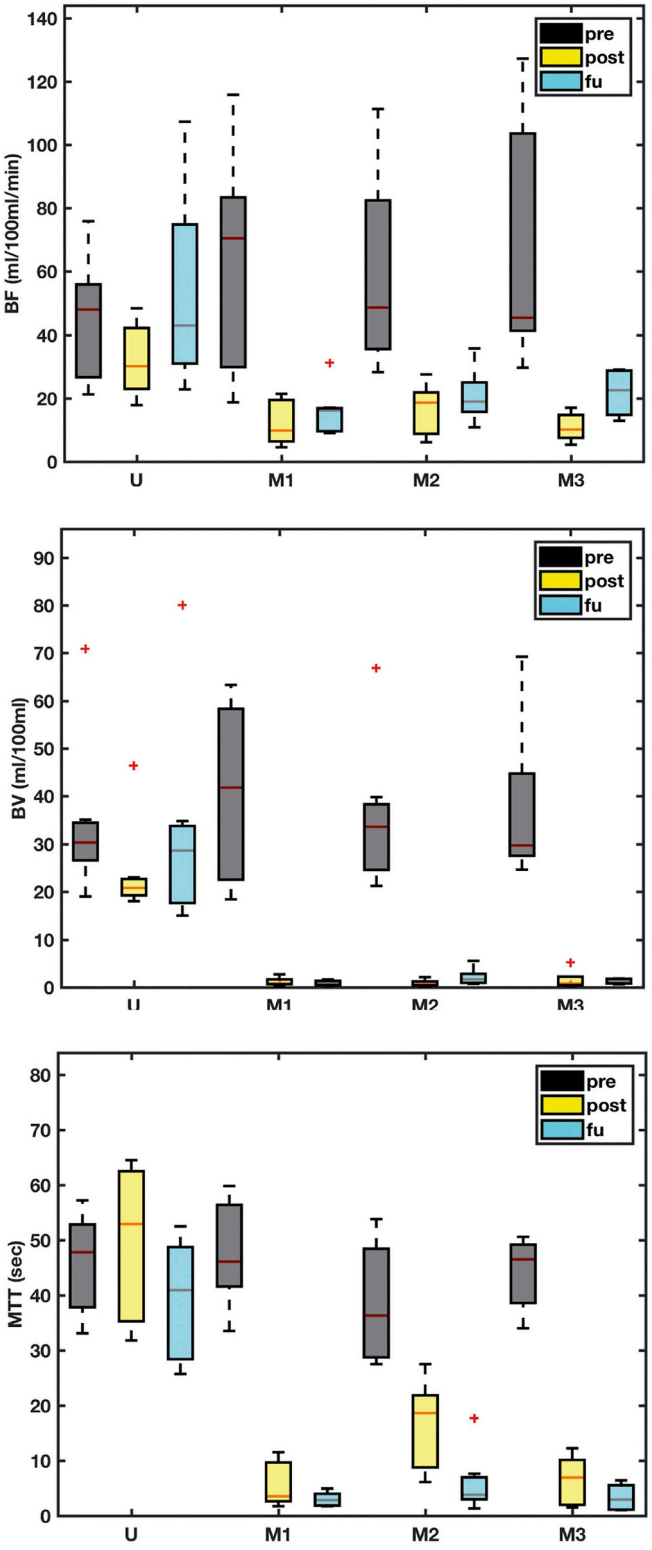

Fig. 4. Boxplots of measured perfusion parameters grouped by time of examination and lesions. Top: blood flow, middle: blood volume, bottom: mean transit times. Time points color coded: black = pre-intervention, yellow = post-intervention, and magenta = follow-up. The central mark (red line) in the box depicts the median value and the boxes top and bottom edges the 25th and 75th percentiles of the data, respectively. The whiskers extend to the most extreme data points not considering outliers which are depicted by '+'. While for myomas (M1–M3) after embolization a change in all parameters could be observed, healthy uterus tissue (U) recovered. (For interpretation of the references to color in this figure legend, the reader is referred to the web version of this article.)

Moreover, in this study, we only applied a deconvolution approach for quantification of the perfusion parameters. Currently, if a patient is examined by DCE-MRI, the Toſts model is most widely used in clinical routine [38]. However, various other perfusion models exist and no consensus on the pharmacokinetic model is yet reached [39]. Gaa et al. compared the deconvolution approach to model based pharmacokinetic models in rectal cancer and found no significant differences in the obtained models [40]. Therefore, in the light of showing the feasibility of our approach, a deconvolution approach seems reasonable. A comparison of pharmacokinetic models remains future work.

5. Conclusion

When performed by an experienced team superselective positioning of the microcatheter targeting the arterial supply of the myoma is possible without the risk of dislocation of embolic material. Our results could clearly demonstrate devascularization of symptomatic uterus myomas (significantly reduced perfusion values) which correlated with cessation of hypermenorrhea in all treated patients without affecting healthy uterus tissue (perfusion values remain). Supplementing UAE with quantitative perfusion imaging to monitor early treatment response is feasible and might provide valuable information for the follow-up of patients and might contribute to providing confidence for the patients in treatment success.

Conflict of interest

The authors declare no competing interests.

References

[1] Lumsden MA, Wallace EM. Clinical presentation of uterine fibroids. Baillieres Clin Obstet Gynaecol 1998;12(2):177–95.
[2] Stewart EA, Cookson CL, Gandolfo RA, Schulze-Rath R. Epidemiology of uterine fibroids: a systematic review. BJOG. 2017;124(10):1501–12.
[3] Buttram Jr. VC, Reiter RC. Uterine leiomyomata: etiology, symptomatology, and management. Fertil Steril 1981;36(4):433–45.
[4] Gupta S, Jose J, Manyonda I. Clinical presentation of fibroids. Best Pract Res Clin Obstet Gynaecol 2008;22(4):615–26.
[5] Shen Y, Xu Q, Xu J, Ren ML, Cai YL. Environmental exposure and risk of uterine leiomyoma: an epidemiologic survey. Eur Rev Med Pharmacol Sci 2013;17(23):3249–56.
[6] Rey VE, Labrador R, Falcon M, Garcia-Benitez JL. Transvaginal radiofrequency ablation of myomas: technique, outcomes, and complications. J Laparoendosc Adv Surg Tech A 2019;29(1):24–8. https://doi.org/10.1089/lap.2018.0293.
[7] Ruhnke H, Eckey T, Bohlmann MK, Beldoch MP, Neumann A, Agic A, et al. MR-guided HIFU treatment of symptomatic uterine fibroids using novel feedback-regulated volumetric ablation: effectiveness and clinical practice. RöFo 2013;184(10):983–91.
[8] Jung SG, Yoon SW, Park H, Lee C. Potential exploratory use of MR-guided focused ultrasound for disconnection of symptomatic intracavitary submucosal uterine myoma. J Vasc Interv Radiol 2011;22(11):1635–7.
[9] Ravina JH, Herbreteau D, Ciraru-Vigneron N, Bouret JM, Houdart E, Aymard A, et al. Arterial embolisation to treat uterine myomata. Lancet. 1995;346(8976):671–2.
[10] Rabe T, Saenger N, Ebert AD, Roemer T, Tinneberg HR, De Wilde RL, et al. Selective progesterone receptor modulators for the medical treatment of uterine fibroids with a focus on ulipristal acetate. Biomed Res Int 2018;2018:1374821.
[11] Esmya: new measures to minimise risk of rare but serious liver injury (2018).
[12] Lurie S, Piper I, Woliovitch I, Glezerman M. Age-related prevalence of sonographicaly confirmed uterine myomas. J Obstet Gynaecol 2005;25(1):42–4.
[13] Lee MS, Kim MD, Jung DC, Lee M, Won JY, Park SI, et al. Apparent diffusion coefficient of uterine leiomyoma as a predictor of the potential response to uterine artery embolization. J Vasc Interv Radiol 2013;24(9):1361–5.
[14] Cao MQ, Suo ST, Zhang XB, Zhong YC, Zhuang ZG, Cheng JJ, et al. Entropy of T2-weighted imaging combined with apparent diffusion coefficient in prediction of uterine leiomyoma volume response after uterine artery embolization. Acad Radiol 2014;21(4):437–44.
[15] Kirby JM, Burrows D, Haider E, Maizlin Z, Midia M. Utility of MRI before and after uterine fibroid embolization: why to do it and what to look for. Cardiovasc Intervent Radiol 2011;34(4):705–16.
[16] Murase E, Siegelman ES, Outwater EK, Perez-Jaffe LA, Tureck RW. Uterine leiomyomas: histopathologic features, MR imaging findings, differential diagnosis, and treatment. Radiographics 1999;19(5):1179–97.
[17] Pelage JP, Guaou NG, Jha RC, Ascher SM, Spies JB. Uterine fibroid tumors: long-term MR imaging outcome after embolization. Radiology 2004;230(3):803–9.

[18] Bao G, Hu L, Charles HW, Deipolyi AR. Ineffectiveness of magnetic resonance imaging enhancement to predict fibroid volume reduction after uterine artery embolization. Proc (Bayl Univ Med Cent) 2017;30(3):259–61.
[19] Deipolyi A. MRI enhancement predicting fibroid volume reduction to uterine artery embolization. Front Women's Health 2017;2(2):1–3.
[20] Scheurig-Muenkler C, Koesters C, Powerski MJ, Grieser C, Froeling V, Kroencke TJ. Clinical long-term outcome after uterine artery embolization: sustained symptom control and improvement of quality of life. J Vasc Interv Radiol 2013;24(6):765–71.
[21] Goodwin SC, Spies JB, Worthington-Kirsch R, Peterson E, Pron G, Li S, et al. Uterine artery embolization for treatment of leiomyomata: long-term outcomes from the FIBROID Registry. Obstet Gynecol 2008;111(1):22–33.
[22] Li W, Brophy DP, Chen Q, Edelman RR, Prasad PV. Semiquantitative assessment of uterine perfusion using first pass dynamic contrast-enhanced MR imaging for patients treated with uterine fibroid embolization. J Magn Reson Imaging 2000;12(6):1004–8.
[23] Song T, Laine AF, Chen Q, Rusinek H, Bokacheva L, Lim RP, et al. Optimal k-space sampling for dynamic contrast-enhanced MRI with an application to MR renography. Magn Reson Med 2009;61(5):1242–8.
[24] Zöllner FG, Daab M, Sourbron SP, Schad LR, Schoenberg SO, Weisser G. An open source software for analysis of dynamic contrast enhanced magnetic resonance images: UMMPerfusion revisited. BMC Med Imaging 2016;16:7.
[25] Dujardin M, Sourbron S, Luypaert R, Verbeelen D, Stadnik T. Quantification of renal perfusion and function on a voxel-by-voxel basis: a feasibility study. Magn Reson Med 2005;54(4):841–9.
[26] Kruskal WH, Wallis WA. Use of ranks in one-criterion variance analysis. J Am Stat Assoc 1952;47(260):583–621.
[27] Friedman M. The use of ranks to avoid the assumption of normality implicit in the analysis of variance. J Am Stat Assoc 1937;32(200):675–701.
[28] Hochberg Yosef, Tamhane Ajit C. Multiple Comparison Procedures. Wiley Series in Probability and Statistics John Wiley & Sons, Inc.9780471822226; 1987. https://doi.org/10.1002/9780470316672. (21 September).
[29] Faul F, Erdfelder E, Buchner A, Lang A-G. Statistical power analyses using G*Power 3.1: tests for correlation and regression analyses. Behav Res Methods 2009;41:1149–60.
[30] Fan M, Wu G, Cheng H, Zhang J, Shao G, Li L. Radiomic analysis of DCE-MRI for prediction of response to neoadjuvant chemotherapy in breast cancer patients. Eur J Radiol 2017;94:140–7.
[31] Chapiro J, Duran R, Lin M, Schernthaner R, Lesage D, Wang Z, et al. Early survival prediction after intra-arterial therapies: a 3D quantitative MRI assessment of tumour response after TACE or radioembolization of colorectal cancer metastases to the liver. Eur Radiol 2015;25(7):1993–2003.
[32] Walker-Samuel S, Leach MO, Collins DJ. Evaluation of response to treatment using DCE-MRI: the relationship between initial area under the gadolinium curve (IAUGC) and quantitative pharmacokinetic analysis. Phys Med Biol 2006;51(14):3593–602.
[33] Thorwarth D, Notohamiprodjo M, Zips D, Muller AC. Personalized precision radiotherapy by integration of multi-parametric functional and biological imaging in prostate cancer: a feasibility study. Z Med Phys 2017;27(1):21–30.
[34] Di Stasi C, Cina A, Rosella F, Paladini A, Amoroso S, Romualdi D, et al. Uterine fibroid embolization efficacy and safety: 15 years experience in an elevated turnout rate center. Radiol Med 2018;123(5):385–97. https://doi.org/10.1007/s11547-017-0843-6.
[35] Cao M, Qian L, Zhang X, Suo X, Lu Q, Zhao H, et al. Monitoring leiomyoma response to uterine artery embolization using diffusion and perfusion indices from diffusion-weighted imaging. Biomed Res Int 2017;2017:3805073.
[36] Duvnjak S, Ravn P, Green A, Andersen PE. Magnetic resonance signal intensity ratio measurement before uterine artery embolization: ability to predict fibroid size reduction. Cardiovasc Intervent Radiol 2017;40(12):1839–44.
[37] Kim YS, Kim BG, Rhim H, Bae DS, Lee JW, Kim TJ, et al. Uterine fibroids: semiquantitative perfusion MR imaging parameters associated with the intraprocedural and immediate postprocedural treatment efficiencies of MR imaging-guided high-intensity focused ultrasound ablation. Radiology. 2014;273(2):462–71.
[38] Tong T, Sun Y, Gollub MJ, Peng W, Cai S, Zhang Z, et al. Dynamic contrast-enhanced MRI: use in predicting pathological complete response to neoadjuvant chemoradiation in locally advanced rectal cancer. J Magn Reson Imaging 2015;42(3):673–80.
[39] Ingrisch M, Sourbron S. Tracer-kinetic modeling of dynamic contrast-enhanced MRI and CT: a primer. J Pharmacokinet Pharmacodyn 2013;40(3):281–300.
[40] Gaa T, Neumann W, Sudarski S, Attenberger UI, Schonberg SO, Schad LR, et al. Comparison of perfusion models for quantitative T1 weighted DCE-MRI of rectal cancer. Sci Rep 2017;7(1):12036.